Future Technology
Open Access Journal
ISSN 2832-0379

August 2024| Volume 03 | Issue 03 | Pages 20- 32

Journal homepage: https://fupubco.com/futech

https://doi.org/10.55670/fpll.futech.3.3.4

Future Publishing LLC

Article

The comparative performance study of the EF7 downsized engines; fuel economy besides CO_2 reduction

Mohammad Mostafa Namar[1]*, Omid Jahanian[2], Kamyar Nikzadfar[3], Rouzbeh Shafaghat[2]

[1]University of Science and Technology of Mazandaran, Behshahr, Iran
[2]Babol Noshirvani University of Technology, Babol, Iran
[3]University of Warwick, Coventry, UK

ARTICLE INFO

Article history:
Received 10 April 2024
Received in revised form
12 May 2024
Accepted 28 May 2024

Keywords:
Engine downsizing, Engine performance, fuel consumption, CO_2, EF7

*Corresponding author
Email address:
m.namar@stu.nit.ac.ir

DOI: 10.55670/fpll.futech.3.3.4

ABSTRACT

Engine downsizing is considered a strategic idea in fuel economy enhancement as well as CO_2 reduction. It is defined in the literature as the decrease in engine geometrical dimensions besides its performance being fixed. In this research, the Iranian gasoline-fueled national engine, EF7, has been investigated for 25% downsizing. After introducing the gasoline-fueled and CNG-fueled versions of downsized engines, their performance, besides CO_2 release rates are studied in detail. A one-dimensional engine simulator coupled with a 3D-CFD model is developed to carry out such an investigation, an experimental test setup is provided to evaluate the accuracy of the provided numerical model, as well. The first version of presented downsized engines, called EF7α, is a 3-cylinder engine with the same geometrical characteristics as the base engine, which is equipped with a turbo-charger and dual CVVT technologies. The EF7β is then introduced by fuel shifting to CNG as the second version of downsized engines, and finally, increasing the compression ratio, the EF7γ is presented as the third version of studied-downsized engines. The results show almost the same rate of BSFC besides a 3.4% reduction in CO_2 concentration for EF7α, 20.6% fuel economy enhancement, besides 20.8% reduction in the specific CO_2 release rate for EF7β, and 28.8% fuel economy enhancement, besides 25.3% reduction in the specific CO_2 release rate for EF7γ in comparison with the base engine.

1. Introduction

Nowadays, fuel economy and cleaner production are two key factors in developed engines as well as conventional performance parameters such as power-to-weight ratio, maximum provided torque range, and Brake Mean Effective Pressure (BMEP) [1-2]. In addition to the well-known emissions, the greenhouse gases, especially CO_2, are now considered to be reduced as the main source of global warming in the automotive industry [3-4]. Although a wide range of strategies [5-6] has been employed to achieve this aim, engine downsizing is considered as the most efficient way to enhance the fuel economy and CO_2 reduction. The idea of engine downsizing refers to the decline in the engine's geometrical dimensions, besides its performance, which is kept fixed [7]. Such behavior from downsized engines would be applicable when employing engine boost technologies such as Turbo-Charger (TC) [8], Direct Injection (DI) [9], and Variable Valve Timing (VVT) [10]. In this case, the fuel consumed to provide the same torque and power would be reduced, as well as the engine's total weight [11]. Consequently, the Brake Specific Fuel Consumption (BSFC) and CO_2 production rate will decrease, and the engine's power-to-weight ratio will increase [12]. Although the concept of engine downsizing has been expressed since the 1990s [13-15]; the concentrated efforts for designing and developing downsized engines have flourished since 2011 [16] when the long-term goal of the International Energy Agency (IEA) was published, suggesting 50% reduction in CO_2 until 2030 [17]. These efforts caused a 32% reduction in fuel consumption in European markets until 2015 [18], and mainly focused on Spark Ignition (SI) rather than Compression Ignition (CI) engines [12]. After releasing the primary versions of downsized engines, well-known strategies in the literature for engine performance enhancement were soon introduced on the downsized versions. Using modified inlet components design [19],

developed TC such as Variable Geometric Turbines (VGT) [20] and twin-turbines [21], improved injection strategy [22], water injection [23], employing additives [24], combined [25] and alternative [26] fuels, Exhaust Gas Recirculation (EGR) [27], and electrified components [28] are considered as the some of these techniques. It is asserted that both fuel economy and CO_2 production rate are noticeably improved during these efforts, but some challenging issues such as knock [29] and super-knock [30], Low-Speed Pre-Ignition (LSPI) [31], and weak performance especially at low-speed regions [32] are the main obstacles which researchers try to cope with them. Indeed, to achieve the ultra-emission reduction goal, the efforts lead to the usage of Compressed Natural Gas (CNG) as the fuel of downsized engines [33-35]. The performance loss due to the lower-combustion characteristics of CNG in comparison with gasoline is expected, and researchers have suggested different strategies such as increasing the Compression Ratio (CR) [36], Octane number enhancement [37], and direct injection [38-40] to improve the performance of these kinds of downsized engines. However, the weak performance of CNG-fueled downsized engines in comparison with the base engine is still reported in the literature [36-40]. In this research, the performance analysis of both gasoline-fueled and CNG-fueled downsized engines from Naturally Aspirated (NA) EF7 engines is presented. Although the performance and emission analysis of the gasoline-fueled version of the downsized engine are presented, the main novelty of this work is the performance enhancement of GNG-fueled ones at low-speed regions. The main strategy of downsizing is removing a cylinder from the base engine, providing a 3-cylinder engine, besides employing boosted technologies namely TC, dual CVVT, and increasing the CR, simultaneously. To carry out such an investigation, a coupled one-dimensional (1D) engine simulator with a three-dimensional Computational Fluid Dynamics (3D-CFD) model is developed, and an experimental test setup is also provided to evaluate the model's accuracy.

2. Model description

A 1D engine simulator had been provided previously by the authors to estimate the performance of the downsized engines as well as the right-sized ones [41-42]. In this simulator, the engine open cycle is simulated, and each component is modeled by the 1D-CFD simulation. The main characteristics of the working fluid, namely the pressure, temperature, and mass flow rate, are calculated alongside the length of each component, and the engine closed cycle between Inlet Valve Closing (IVC) and Exhaust Valve Opening (EVO) is simulated by the 0D two-zone thermodynamically sub-model. This sub-model estimates the rate of heat release due to the burnt fuel mass fraction, which is calculated by the developed Wiebe function for both gasoline and CNG blends:

$$x_b = 1 - \exp\left(-Ea\left(\frac{\theta-\theta_{ig}}{\Delta\theta}\right)^{m+1}\right) \quad (1)$$

Here, x_b, E_a, and θ_{ig} are the mass fraction of burnt fuel, activation energy, and spark time, respectively.

In this work, a 3D-CFD model of an engine closed cycle is coupled with a 1D engine simulator to enhance the accuracy of engine performance evaluation as well as engine emission calculation. The characteristics of charge at IVC from the 1D model are employed as the initial conditions for the 3D-CFD model, and then, the rate of heat release from the 3D-CFD model is used instead of the Wiebe function at the 1D simulator. Furthermore, the results of engine emission from the 3D-CFD model are employed to calibrate the emissions sub-models of the 1D simulator. Figure 1 shows how the 1D simulator is coupled with the 3D-CFD model. The details of employed correlations at the 1D simulator and 3D-CFD model are presented in [41-43].

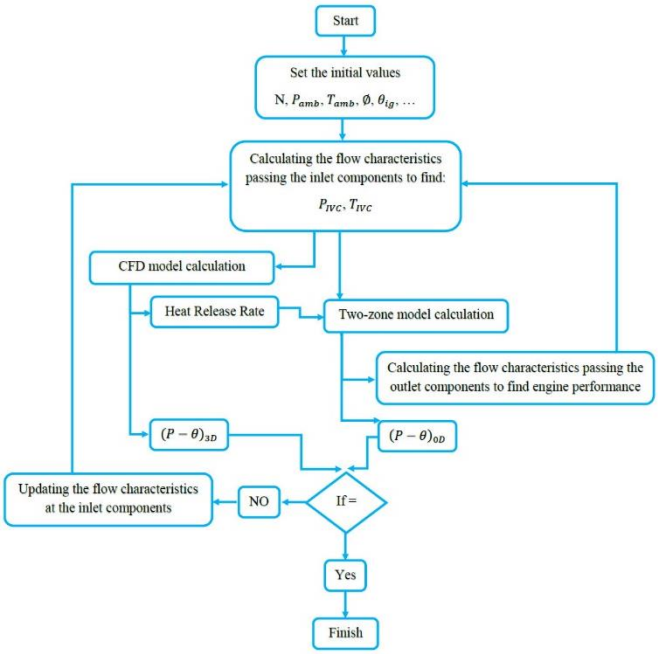

Figure 1. The schematic of coupled 1D simulator with 3D-CFD model

3. Experimental test setup

The gasoline-fueled EF7NA and bi-fuel EF7TC engines are employed for both validation of the model and estimation of the performance of downsized engines. The main characteristics of the engines are reported in Table 1. The EF7TC engine is able to run on gasoline or CNG, and the experimental results of each mode are considered for the validation study at the first step. Then, to evaluate the performance of downsized engines, the configuration of EF7TC is shifted to the cylinder-deactivated mode. The fuel injector of the target cylinder is deactivated, and the amount of fuel injected into the other 3 cylinders is kept fixed thanks to the use of an open Electronic Control Unit (ECU). In this case, the equivalence ratio of each active cylinder is considered the same as the standard condition defined by the producer for normal EF7TC, and the achieved performance can be considered as the 3-cylinder engine performance after reducing the losses due to the deactivated cylinder. However, the engine operation is slightly unbalanced, and the emissions data are unreliable in this situation. More details about the experimental test setup and the accuracy of employed measurement instruments are presented in [42].

4. Validation

Due to de defined aims of this study, as the EF7NA is defined as the base engine and the downsized versions use turbochargers and run with both gasoline and CNG fuels, it is

necessary to verify the results of the model by the experimental results of the base engine as well as the standard TC engine, defined in Table 1. The in-cylinder pressure variation is selected to evaluate the performance of the provided model, as it is considered the basic parameter for engine performance calculation. In Figure 2 (a-c), the results of estimated in-cylinder pressure from both the 1D simulator and 3D-CFD model are compared with experimental results. The detected errors for peak-pressure are 4.1% for EF7NA and less than 1% for EF7TC, as well as the peak-pressure location errors, which are calculated at 4.2 CAD for EF7NA and less than 2 CAD for EF7TC. Such a high-accuracy estimation is achieved by employing the sufficient heat release curve from the 3D-CFD model, which is shown in Figure 2d for EF7NA as an example. It should be noted that, for the 3D-CFD model, a 45° slice of the combustion chamber is considered the solving geometrical domain. The solver shows independent results from the number of employed meshes, considering 12208 cells, and from the time steps of 1 CAD during the compression/expansion course and 0.1 CAD during the combustion course. More details are presented in Appendixes A, B, and C.

Table 1. The main characteristics of EF7NA and EF7TC

Engine Name	EF7NA	EF7TC
Engine Type	4 inline cylinder	
Bore × Stroke	78.6 × 85 mm	
Connection Rod Length	134.5 mm	
Compression Ratio	11	9.6
IVC	40 deg aBDC	26 deg aBDC
EVO	50 deg bBDC	25 deg bBDC
Fuel	Gasoline	Gasoline / CNG
CVVT	Intake	---

To validity check of the predicted emissions, the concentrations of NOx, CO, CO_2, and HC specious are compared via experimental results of gasoline-fueled EF7TC. The high accuracy of simulated results for NOx, CO, and CO_2 prediction are also shown in Figure 3, but due to ignoring some of the geometrical criteria, such as valve sitting area and hotspots, and not considering the chemical-kinetics mechanism of combustion, the estimation of HC is not reliable. In fact, the only specious for HC is assumed to be the residual fuel, which is mainly formed at the gap between the piston and cylinder wall, shown in Appendix D.

5. Results and discussion

Gasoline-fueled EF7NA is considered the base engine, and the downsized versions will be compared with its performance of it. To ensure that the downsized versions are able to provide the performance at least the same as the base engine, full load conditions are the worst case.

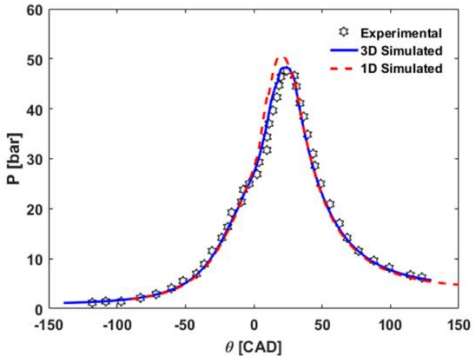

(a)

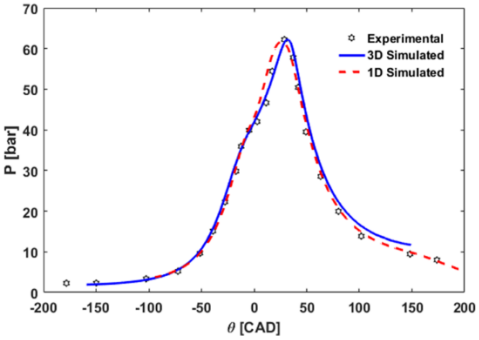

(b)

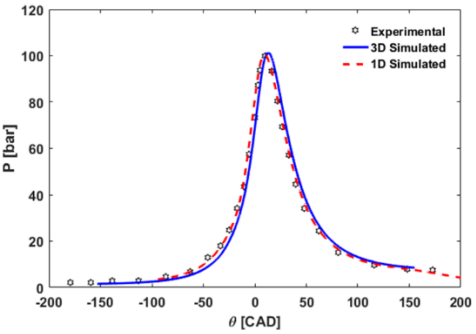

(c)

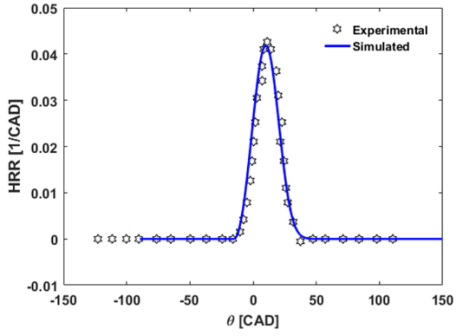

(d)

Figure 2. In-cylinder pressure variation for a) EF7NA, N=3000rpm, Ø=1.12, Ig=5.3bTDC b) Gasoline-fueled EF7TC, N=5500rpm, Ø=1.37, Ig=11.5bTDC c) CNG-fueled EF7TC, N=5500rpm, Ø=1.07, Ig=35.6bTDC d)Heat Release Rate for EF7NA, N=3000rpm, Ø=1.12, Ig=5.3bTDC

Consequently, the analysis of this study was carried out under full-load conditions. The performance curves of the base engine are shown in Figure 4. EF7NA is able to provide the maximum torque of 145 Nm at 3000 to 5000 rpm, and in the case of 1000 rpm, it presents 114 Nm torque. The minimum range of BSFC is reported by 275g/kWh between 2000 and 3000 rpm, and the concentration of released CO_2 finds its maximum value at 1500 rpm by 130232 ppm. The amount of CO_2 emission is slightly reduced during the sweep of engine speed due to the engine operating condition. At full load conditions, the richness of the charge increases via engine speed to prevent the engine from knocking. In this case, un-stoichiometric combustion leads to more CO and HC, besides less CO_2.

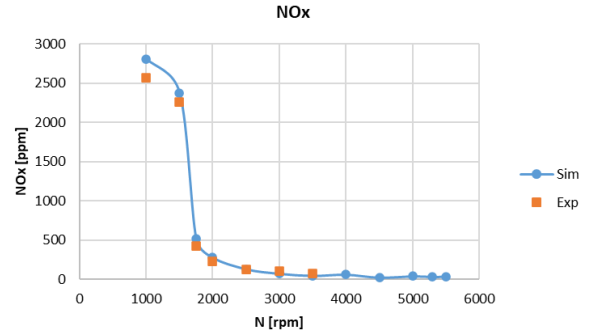

(a)

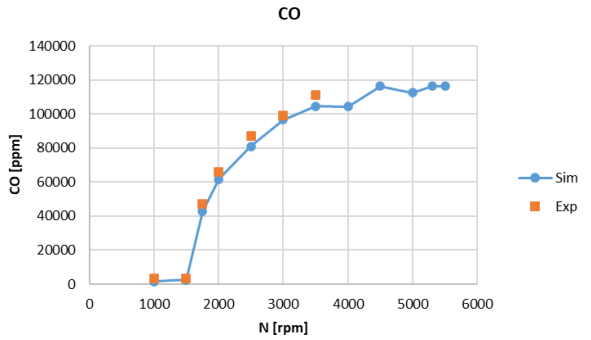

(b)

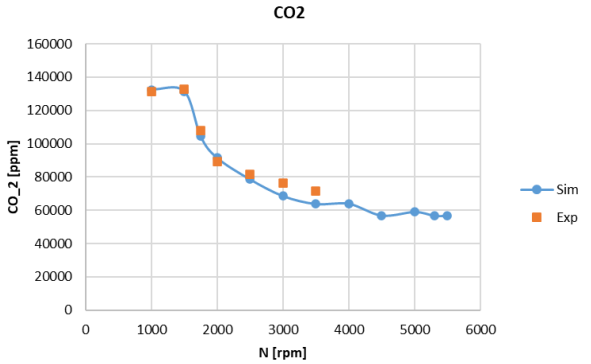

(c)

Figure 3. a) NO_x b) CO and c) CO_2 variation for gasoline-fueled EF7TC, full load condition

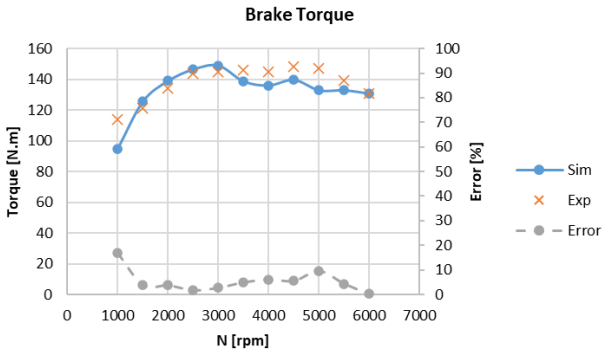

(a)

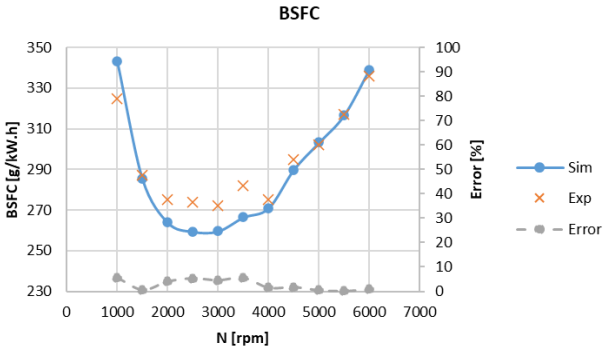

(b)

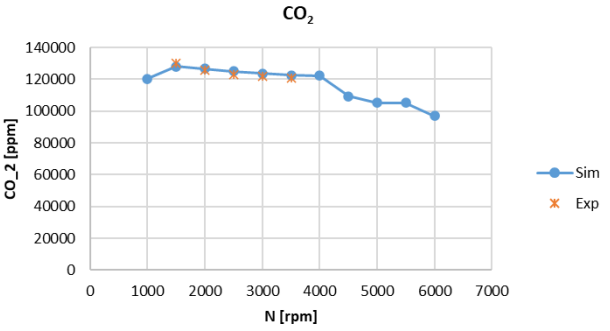

(c)

Figure 4. Full load performance of EF7NA, a) Torque, b) BSFC, c) CO_2

The first version of the downsized engine from EF7NA, called EF7α, is a 33-cylinder turbocharged engine that is equipped with dual CVVT. The main characteristics of EF7α in comparison with the base engine and other downsized versions are reported in Table 2. The steps for improving the performance of EF7α are illustrated in detail in [42]. However, using a matched turbocharger besides optimum valve timing in low-speed regions is able to provide the torque the same as the base engine after 1500 rpm, as shown in Figure 5. In the case of 1000 rpm, the provided torque by the EF7α is just 7.1% less than the base engine. The maximum torque provided is enhanced by 15 Nm to 160 Nm in comparison with the base engine, and the maximum torque range is extended to 2500 rpm. The trend of BSFC variation can be divided into two sections, before and after 3500 rpm.

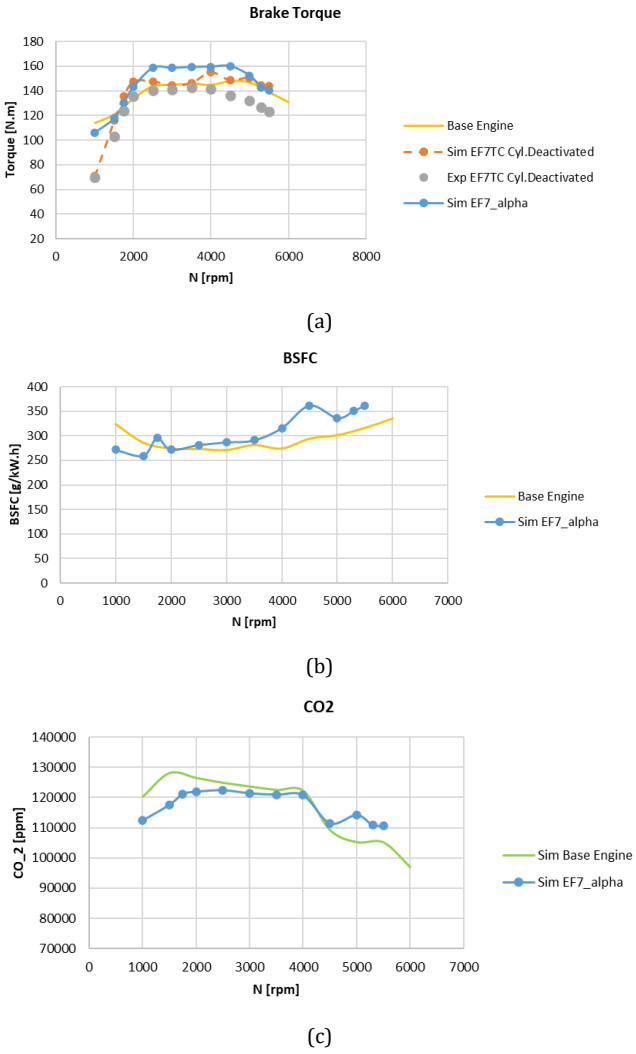

Figure 5. Full load performance of EF7α, a) Torque, b) BSFC, c) CO_2

The estimated BSFC before 3500 rpm shows the same value as the base engine due to the same increased percentage of both provided power and consumed fuel, while the provided power is decreased sharply after that. In the case of 1000 rpm, the BSFC of EF7α is 16.4% less than the base engine. The main effective parameters of the released CO_2 are the volumetric efficiency enhancement due to the boosted charge pressure, which leads to more consumed fuel, and CO_2 formation and the removed volume of a cylinder, which has the opposite effect. The superposition of these changes caused a 3.4% reduction in CO_2 concentration between 1000 and 4000 rpm. It should be noted that to have an experimental evaluation of the performance of downsized engines, the fuel cut-off strategy is applied to a cylinder of EF7TC, which is called cylinder deactivated in this work.

EF7β is the second version of investigated downsized engines. The fuel of EF7α is shifted to the CNG, and the spark time is set to achieve acceptable performance. More details about the spark time selection criteria for this engine are available in the authors' previous published work [41]. EF7β is able to provide the torque as same as the base engine after 2000 rpm, as shown in Figure 6.

Table 2. The main characteristics of base and downsized engines

Engine Name	Base Engine	EF7α	EF7β	EF7γ
Engine Type	4 inline cylinders	3 inline cylinders		
	NA	TC		
Bore × Stroke	78.6×85 mm			
Connection Rod Length	134.5 mm			
Compression Ratio	11	9.6	9.6	12.2
Fuel	gasoline	gasoline	CNG	CNG
CVVT	Intake	Intake + Exhaust		

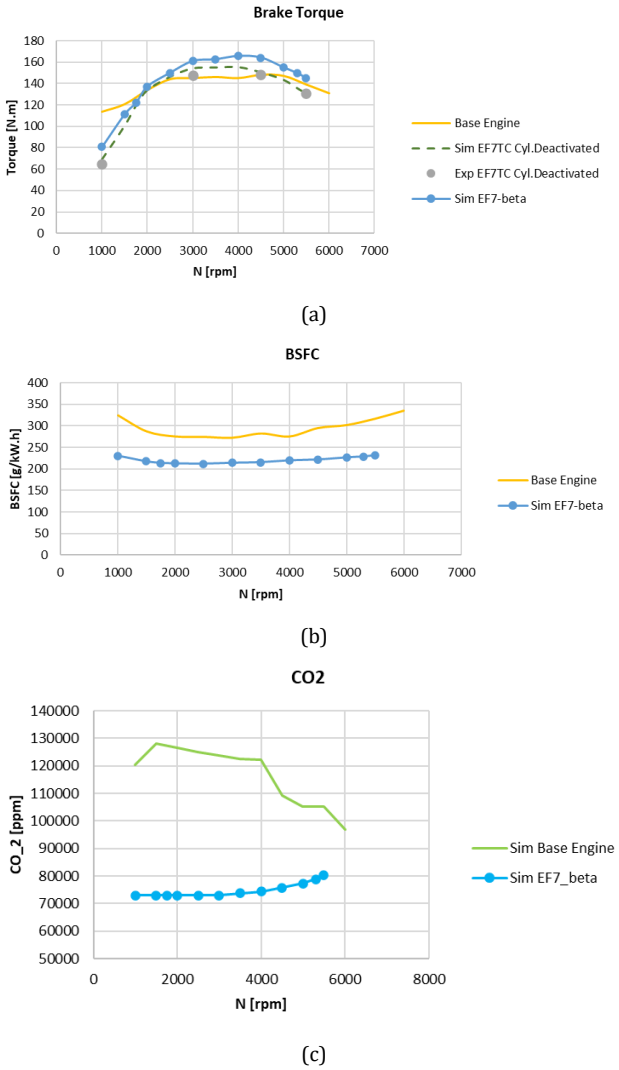

Figure 6. Full load performance of EF7β, a) Torque, b) BSFC, c) CO_2

Although in the case of 1000 rpm, the provided torque by the EF7β is 29.8% less than the base engine, its performance is acceptable after 1500 rpm. Using the lighter hydrocarbon as the fuel, BSFC and CO_2 concentration are meanly 24% and 36.7% reduced, respectively. Here, the trend of CO_2 concentration is due to stoichiometric combustion with no concern about the knock during the entire range of engine speed. More fuel is needed at high speed as the inlet air mass flow rate increases. Considering the high anti-knock index of CNG as the fuel, the compression ratio of EF7β is modified to 12.2, and the third version of the downsized engine is introduced as EF7γ. This engine is able to provide the same torque as the base engine after 1500 rpm, as shown in Figure 7. In the case of 1000 rpm, the provided torque by the EF7γ is just 13.1% less than the base engine, and provided maximum torque is enhanced to 190 N.m in comparison with the base engine. Indeed, BSFC and CO_2 concentration are meanly 31% and 35.6% reduced, respectively. It should be noted that operating with such a compression ratio means the engine temperature would be increased, so the optimal design of the components and engine calibration will be needed.

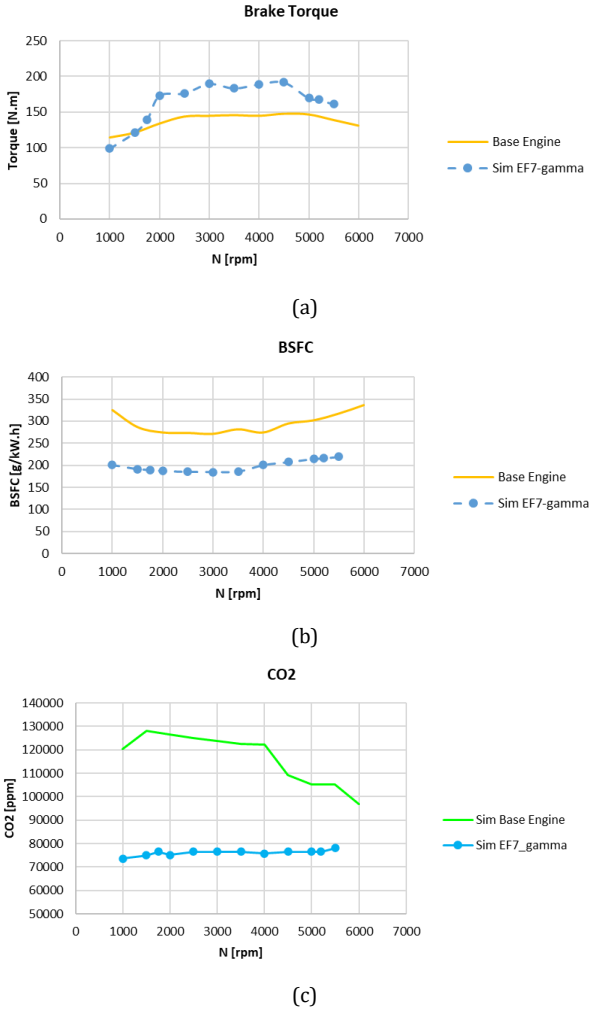

Figure 7. Full load performance of EF7γ, a) Torque, b) BSFC, c) CO_2

A comparison of the torque provided by the introduced downsized engines is presented in Figure 8. Both of EF7α and EF7γ provide acceptable performance during all ranges of engine speeds. All 3 versions, especially EF7γ provide the maximum torque noticeably more than the base engine in the wide range of operating condition, in consequent, the design of engines can be modified to the lean burnt and achieve less fuel consumption besides emission reduction.

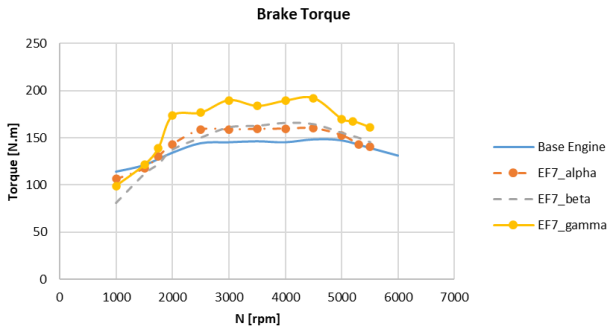

Figure 8. Provided torque by the downsized engines

Having a real comparison of fuel economy, the cost of BSFC is compared for the studied engines, as shown in Figure 9. Considering 2.19 and 2.32 $/Gallon for CNG and gasoline, respectively, the cost of fuel consumed per provided power is shown to be almost the same amount for EF7α in comparison with the base engine. However, the fuel economy of this engine for low-speed regions, less than 200 rpm, is a promising point as the EURO-6 emission standard follows the WLTC driving cycle, which leads the engine to operate more in low-speed full-load conditions. In addition, EF7β and EF7γ improve the fuel economy by meanly 20.6% and 28.8%, respectively, thanks to using CNG as the fuel.

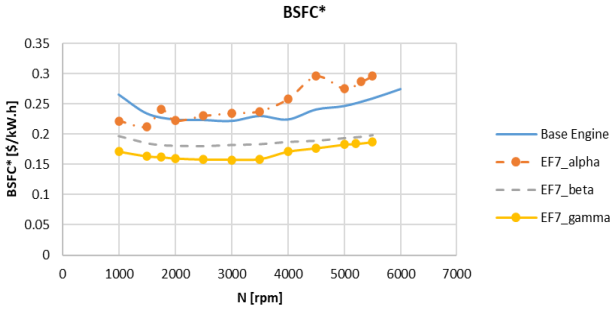

Figure 9. The cost of BSFC of the downsized engines

To present a realistic analysis of released CO_2, the specific emission rates of studied engines are compared in Figure 10. The comparison of CO_2 emission based on the concentration, ignores the effect of mass flow rate, in conclusion, the mass of released CO_2 per provided power is considered as the criterion of such a comparison. In this case, EF7α produces a meanly 21.1% CO_2 more than the base engine, and the released CO_2 for EF7β and EF7γ is meanly 20.8% and 25.3% less than EF7NA.

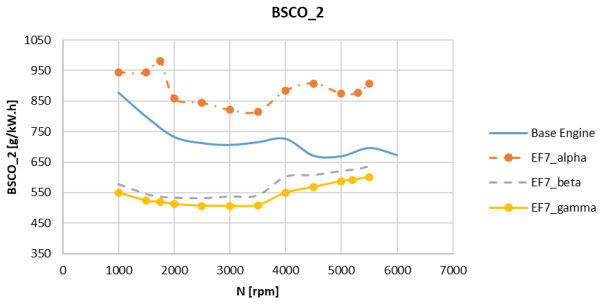

Figure 10. CO_2 specific emission rate of the downsized engines

6. Conclusion

In this research, EF7NA has been investigated for 25% downsizing using the strategy of providing 3-cylinder engines, which are boosted by the turbocharger and dual CVVT. The performance and CO_2 release rates of the downsized engine are studied by presented one-dimensional engine simulator coupled with a 3D-CFD model. The main results of this study are listed in the following:

- The maximum torque of EF7α and EF7β is estimated by 160 N.m, and it's calculated by 190 N.m for EF7γ.
- EF7α shows almost the same rate of BSFC besides 3.4% reduction in CO_2 concentration in comparison with the base engine.
- EF7β shows 20.6% fuel economy enhancement besides 20.8% reduction in the specific CO_2 release rate in comparison with the base engine.
- EF7γ shows 28.8% fuel economy enhancement besides 25.3% reduction in the specific CO_2 release rate in comparison with the base engine.

Ethical issue

The authors are aware of and comply with best practices in publication ethics, specifically with regard to authorship (avoidance of guest authorship), dual submission, manipulation of figures, competing interests, and compliance with policies on research ethics. The authors adhere to publication requirements that the submitted work be original and not published elsewhere.

Data availability statement

The datasets analyzed during the current study are available and can be given upon reasonable request from the corresponding author.

Conflict of interest

The authors declare no potential conflict of interest.

References

[1] Khallaghi, N., Hanak, D.P. and Manovic, V., 2020. Techno-economic evaluation of near-zero CO2 emission gas-fired power generation technologies: A review. Journal of natural gas science and engineering, 74, p.103095. https://doi.org/10.1016/j.jngse.2019.103095

[2] Namar, M.M., Jahanian, O. and Koten, H., 2022. The Start of Combustion Prediction for Methane-Fueled HCCI Engines: Traditional vs. Machine Learning Methods. Mathematical Problems in Engineering, 2022. https://doi.org/10.1155/2022/4589160

[3] Hassan, M.H.A., Sher, F., Zarren, G., Suleiman, N., Tahir, A.A. and Snape, C.E., 2020. Kinetic and thermodynamic evaluation of effective combined promoters for CO2 hydrate formation. Journal of Natural Gas Science and Engineering, 78, p.103313. https://doi.org/10.1016/j.jngse.2020.103313

[4] Namar, M.M., Jahanian, O., Shafaghat, R. and Nikzadfar, K., 2021. Engine Downsizing; Global Approach to Reduce Emissions: A World-Wide Review. HighTech and Innovation Journal, 2(4), pp.384-399. http://dx.doi.org/10.28991/HIJ-2021-02-04-010

[5] Namar, M.M. and Jahanian, O., 2019. Energy and exergy analysis of a hydrogen-fueled HCCI engine. Journal of Thermal Analysis and Calorimetry, 137(1), pp.205-215. https://doi.org/10.1007/s10973-018-7910-7

[6] Namar, M.M. and Jahanian, O., 2017. A simple algebraic model for predicting HCCI auto-ignition timing according to control oriented models requirements. Energy Conversion and Management, 154, pp.38-45. https://doi.org/10.1016/j.enconman.2017.10.056

[7] Jiang, C., Parker, M.C., Butcher, D., Spencer, A., Garner, C.P. and Helie, J., 2019. Comparison of flash boiling resistance of two injector designs and the consequences on downsized gasoline engine emissions. Applied Energy, 254, p.113735. https://doi.org/10.1016/j.apenergy.2019.113735

[8] Millo, F., Luisi, S., Borean, F. and Stroppiana, A., 2014. Numerical and experimental investigation on combustion characteristics of a spark ignition engine with an early intake valve closing load control. Fuel, 121, pp.298-310. https://doi.org/10.1016/j.fuel.2013.12.047

[9] Ma, J. and Zhao, H., 2015. The modeling and design of a boosted uniflow scavenged direct injection gasoline (BUSDIG) engine (No. 2015-01-1970). SAE Technical Paper. https://doi.org/10.4271/2015-01-1970

[10] De Bellis, V., 2016. Performance optimization of a spark-ignition turbocharged VVA engine under knock limited operation. Applied energy, 164, pp.162-174. https://doi.org/10.1016/j.apenergy.2015.11.097

[11] Lang, O., 2004. Turbocharged engine with gasoline direct injection. AutoTechnology, 4(6), pp.56-59. https://doi.org/10.1007/BF03246862

[12] Patil, C., Varade, S. and Wadkar, S., 2017. A Review of Engine Downsizing and its Effects. International Journal of Current Engineering and Technology. Special Issue-7. http://inpressco.com/category/ijcet

[13] Merker, G.P., Schwarz, C. and Teichmann, R. eds., 2011. Combustion engines development: mixture formation, combustion, emissions and simulation. Springer Science & Business Media.

[14] Kuhlbach, K., Mehring, J., Borrmann, D. and Friedfeld, R., 2009. Zylinderkopf mit integriertem Abgaskrümmer für Downsizing-Konzepte. MTZ-Motortechnische Zeitschrift, 70(4), pp.286-293. https://doi.org/10.1007/BF03225480

[15] Smith, A., 2008. Stroke of genius for gasoline downsizing. Ricardo Q Rev, p.Q3.

[16] Ricardo, M.B., Apostolos, P. and Yang, M., 2011. Overview of boosting options for future downsized engines. Science China Technological Sciences, 54(2), pp.318-331. https://doi.org/10.1007/s11431-010-4272-1

[17] International Energy Agency. Policy pathways: improving the fuel economy of road vehicles – A policy package; 2011. http://www.iea.org/publications/freepublications/publication/PP5_Fuel_Economy_FINAL_WEB_Oct_2012.pdf.

[18] Hu, K. and Chen, Y., 2016. Technological growth of fuel efficiency in european automobile market 1975–2015. Energy Policy, 98, pp.142-148. http://dx.doi.org/10.1016/j.enpol.2016.08.024

[19] Budack, R., Wurms, R., Mendl, G. and Heiduk, T., 2016. The New Audi 2.0-l I4 TFSI Engine. MTZ worldwide, 77(5), pp.16-23. https://doi.org/10.1007/s38313-016-0035-0

[20] Serrano, J.R., Piqueras, P., De la Morena, J., Gómez-Vilanova, A. and Guilain, S., 2021. Methodological analysis of variable geometry turbine technology impact on the performance of highly downsized spark-ignition engines. Energy, 215, p.119122. https://doi.org/10.1016/j.energy.2020.119122

[21] Galindo, J., Serrano, J.R., García-Cuevas, L.M. and Medina, N., 2021. Using a CFD analysis of the flow capacity in a twin-entry turbine to develop a simplified physics-based model. Aerospace Science and Technology, 112, p.106623. https://doi.org/10.1016/j.ast.2021.106623

[22] Wei, H., Shao, A., Hua, J., Zhou, L. and Feng, D., 2018. Effects of applying a Miller cycle with split injection on engine performance and knock resistance in a downsized gasoline engine. Fuel, 214, pp.98-107. https://doi.org/10.1016/j.fuel.2017.11.006

[23] Tornatore, C., Siano, D., Marchitto, L., Iacobacci, A., Valentino, G. and Bozza, F., 2017. Water Injection: a Technology to Improve Performance and Emissions of Downsized Turbocharged Spark Ignited Engines. SAE International Journal of Engines, 10(2017-24-0062), pp.2319-2329. https://doi.org/10.4271/2017-24-0062

[24] Corrubia, J.A., Capece, J.M., Cernansky, N.P., Miller, D.L., Durrett, R.P. and Najt, P.M., 2020. RON and MON chemical kinetic modeling derived correlations with ignition delay time for gasoline and octane boosting additives. Combustion and Flame, 219, pp.359-372. https://doi.org/10.1016/j.combustflame.2020.05.002

[25] Sarabi, M. and Aghdam, E.A., 2020. Experimental analysis of in-cylinder combustion characteristics and exhaust gas emissions of gasoline–natural gas dual-fuel combinations in a SI engine. Journal of Thermal Analysis and Calorimetry, 139(5), pp.3165-3178. https://doi.org/10.1007/s10973-019-08727-2

[26] Sun, H., Wang, W. and Koo, K.P., 2021. Application of Methanol as a Clean and Efficient Alternative Fuel for Passenger Cars. In Methanol (pp. 265-282). Springer, Singapore. DOI: 10.1007/978-981-16-1224-4_11

[27] Shen, K., Xu, Z., Chen, H. and Zhang, Z., 2021. Investigation on the EGR effect to further improve fuel economy and emissions effect of Miller cycle turbocharged engine. Energy, 215, p.119116. https://doi.org/10.1016/j.energy.2020.119116

[28] Stoffels, H., Dunstheimer, J. and Hofmann, C., 2017. Potential of Electric Energy Recuperation by Means of the Turbocharger on a Downsized Gasoline Engine (No. 2017-24-0162). SAE Technical Paper. https://doi.org/10.4271/2017-24-0162.

[29] Zhao, X., Zhu, Z., Zheng, Z., Yue, Z., Wang, H. and Yao, M., 2021. Effects of flame propagation speed on knocking and knock-limited combustion in a downsized spark ignition engine. Fuel, 293, p.120407. https://doi.org/10.1016/j.fuel.2021.120407

[30] Gao, J., Yao, A., Zhang, Y., Qu, G., Yao, C., Zhang, S. and Li, D., 2021. Investigation into the Relationship between Super-Knock and Misfires in an SI GDI Engine. Energies, 14(8), p.2099. https://doi.org/10.3390/en14082099

[31] Kar, A., Huisjen, A., Aradi, A., Reitz, J., Iqbal, A., Haumann, K., Kensler, J., Hardman, K., Mainwaring, R. and Remmert, S., 2020. Assessing the Impact of Lubricant and Fuel Composition on LSPI and Emissions in a Turbocharged Gasoline Direct Injection Engine. SAE International Journal of Advances and Current Practices in Mobility, 2(2020-01-0610), pp.2568-2580. https://doi.org/10.4271/2020-01-0610

[32] Ju, K., Kim, J. and Park, J., 2021. Numerical prediction of the performance and emission of downsized two-cylinder diesel engine for range extender considering high boosting, heavy exhaust gas recirculation, and advanced injection timing. Fuel, 302, p.121216. https://doi.org/10.1016/j.fuel.2021.121216

[33] Kar, T., Zhou, Z., Brear, M., Yang, Y., Khosravi, M. and Lacey, J., 2021. A comparative study of directly injected, spark ignition engine performance and emissions with natural gas, gasoline and charge dilution. Fuel, 304, p.121438. https://doi.org/10.1016/j.fuel.2021.121438

[34] Eggenschwiler, P.D., Schreiber, D. and Schröter, K., 2021. Characterization of the emission of particles larger than 10 nm in the exhaust of modern gasoline and CNG light duty vehicles. Fuel, 291, p.120074. https://doi.org/10.1016/j.fuel.2020.120074

[35] Melaika, M., Herbillon, G. and Dahlander, P., 2021. Spark ignition engine performance, standard emissions and particulates using GDI, PFI-CNG and DI-CNG systems. Fuel, 293, p.120454. https://doi.org/10.1016/j.fuel.2021.120454

[36] Streng, S., Wieske, P., Warth, M. and Hall, J., 2016. Monovalent Natural Gas Combustion and Downsizing for Lowest CO2 Emissions. MTZ worldwide, 77(7-8), pp.16-23.

[37] Kramer, U., Lorenz, T., Hofmann, C., Ruhland, H., Klein, R. and Weber, C., 2017. Methane Number Effect on the Efficiency of a Downsized, Dedicated, High Performance Compressed Natural Gas (CNG) Direct Injection Engine (No. 2017-01-0776). SAE Technical Paper. https://doi.org/10.4271/2017-01-0776

[38] Kar, T., 2020. A Study of Compressed Natural Gas Fuelling in a Downsized and Boosted, Multi-Cylinder, Direct Injection Spark-Ignition Engine (Doctoral dissertation).

[39] Dziewiatkowski, M., Szpica, D. and Borawski, A., 2020. Evaluation of impact of combustion engine controller adaptation process on level of exhaust gas emissions in gasoline and compressed natural gas supply process. Engineering for Rural Development, 19, pp.541-548.
[40] Sahoo, S. and Srivastava, D.K., Effect of injection timing on combustion and IMEP variation of a bi-fuel compressed natural gas SI engine. Environmental Progress & Sustainable Energy, p.e13694. https://doi.org/10.1002/ep.13694
[41] Namar, M.M., Jahanian, O., Shafaghat, R. and Nikzadfar, K., 2021. Feasibility Study for Downsizing EF7 Engine, Numerical and Experimental Approach. The Journal of Engine Research, 61(61), pp.73-85. http://engineresearch.ir/article-1-758-en.html
[42] Namar, M.M., Jahanian, O., Shafaghat, R. and Nikzadfar, K., 2021. Numerical/Experimental Studies on Performance at Low Engine Speeds: A Case study Downsized Iranian National Engine (EF7). International Journal of Engineering, 34(9), pp.2137-2147. DOI: 10.5829/ije.2021.34.09c.11
[43] Shamekhi Amiri, S. and Jahanian, O., 2015. Investigation on the Effects of Geometrical Specifications of Injection on Performance of a Direct Injection Hydrogen Fueled Engine. The Journal of Engine Research, 37(37), pp.13-24. http://engineresearch.ir/article-1-457-en.html

Abbreviations

0D	Zero-Dimensional
1D	One-Dimensional
3D	Three-Dimensional
BDC	Bottom Dead Center
BMEP	Brake Mean Effective Pressure, bar
BSFC	Brake Specific Fuel Consumption, g/kWh
CAD	Crank Angle Degree
CFD	Computational Fluid Dynamics
CI	Compression Ignition
CNG	Compressed Natural Gas
CR	Compression Ratio
DI	Direct Injection
ECU	Electronic Control Unit
EGR	Exhaust Gas Recirculation
EVO	Exhaust Valve Opening
IEA	International Energy Agency
IVC	Intake Valve Closing
LSPI	Low Speed Pre-Ignition
NA	Naturally Aspirated
SI	Spark Ignition
TC	Turbo-Charger
TDC	Top Dead Center
VGT	Variable Geometric Turbine
VVT	Variable Valve Timing

English symbols

Ig	Ignition Timing
N	Engine speed, rpm
P	pressure, bar

Greek Symbols

θ	Crank Angle, degree
Ø	Equivalence Ratio

Appendix

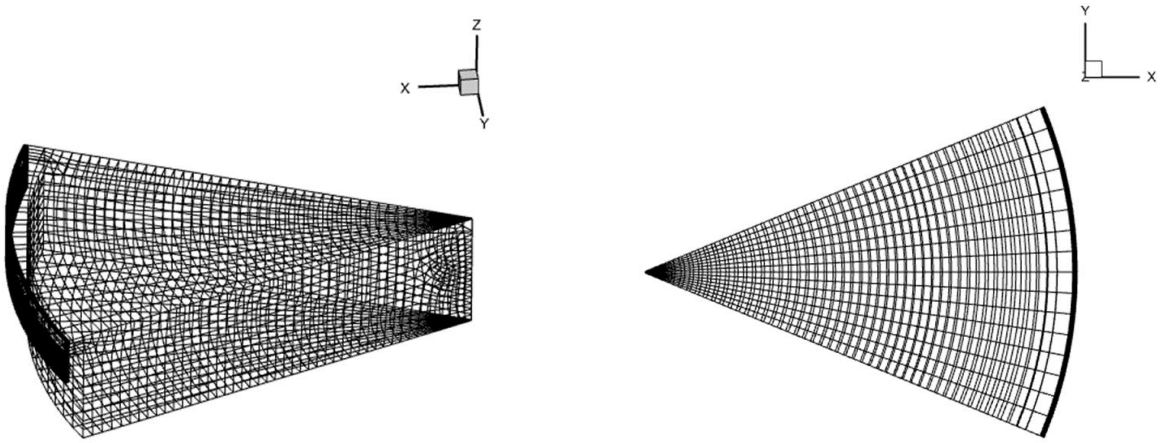

Isometric View Top View

A. Considered solving geometrical domain for 3D-CFD model

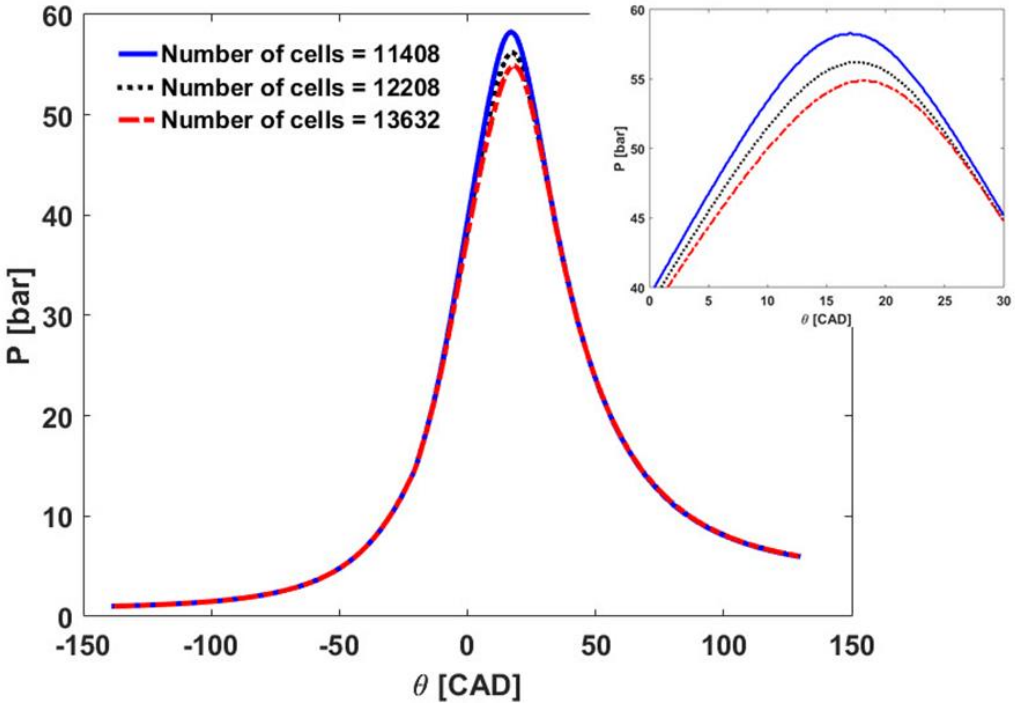

B. Mesh independency for 3D-CFD model

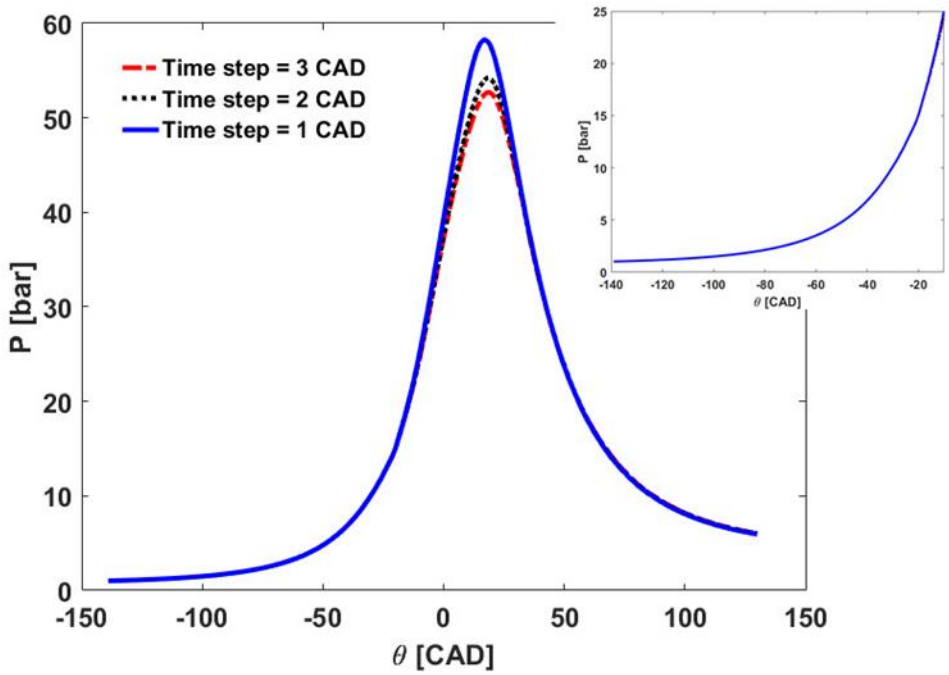

Compression/Expansion

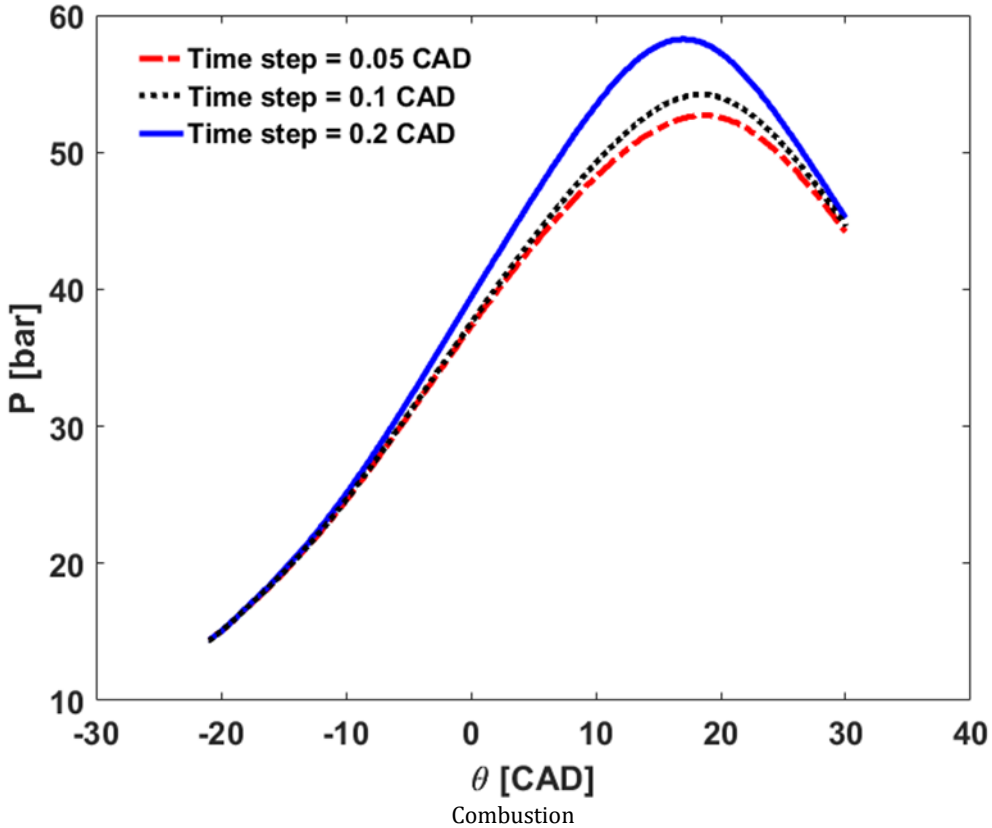

Combustion

C. Time step independence for 3D-CFD model

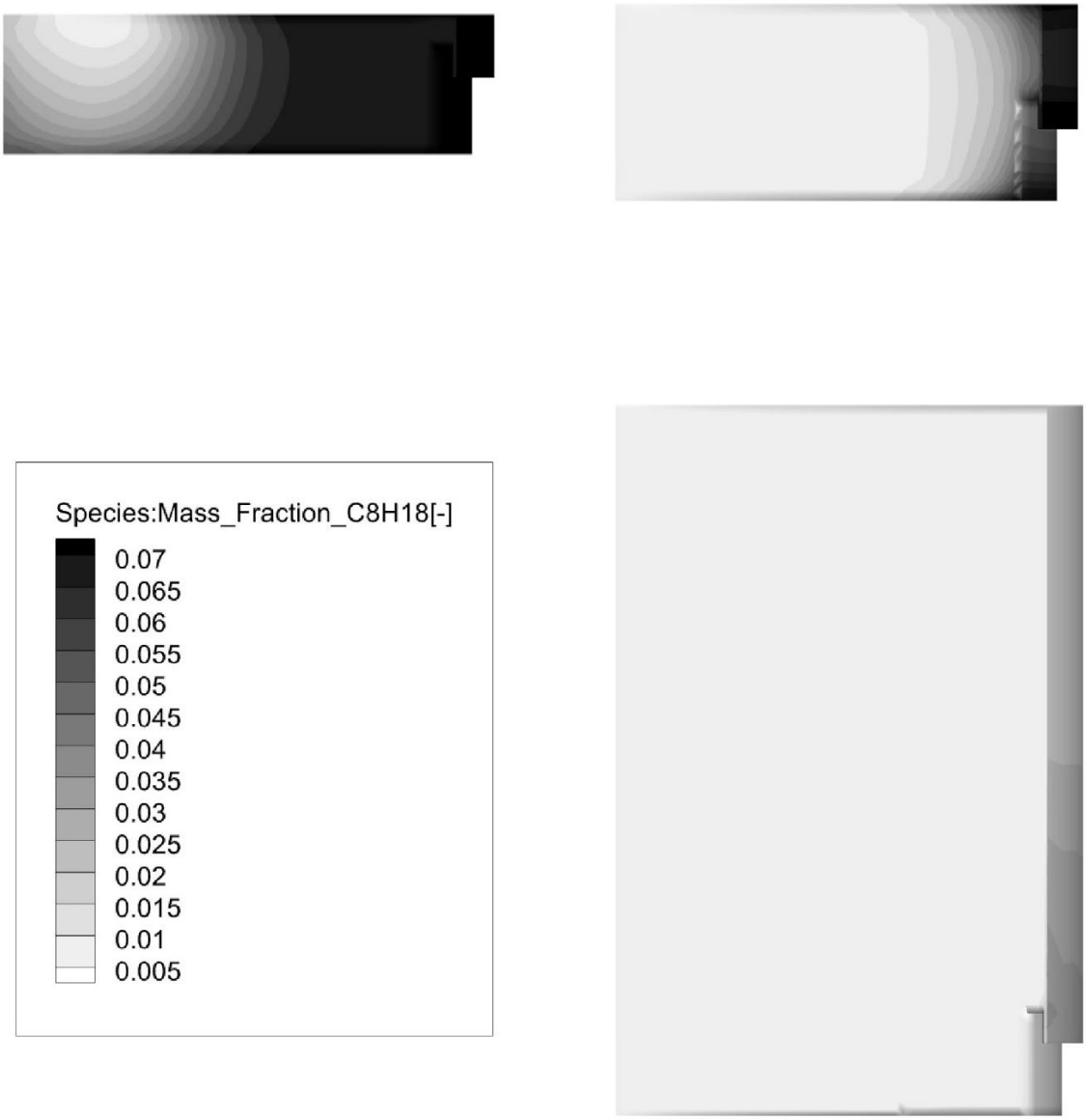

D. Considered area for HC formation by the 3D-CFD model

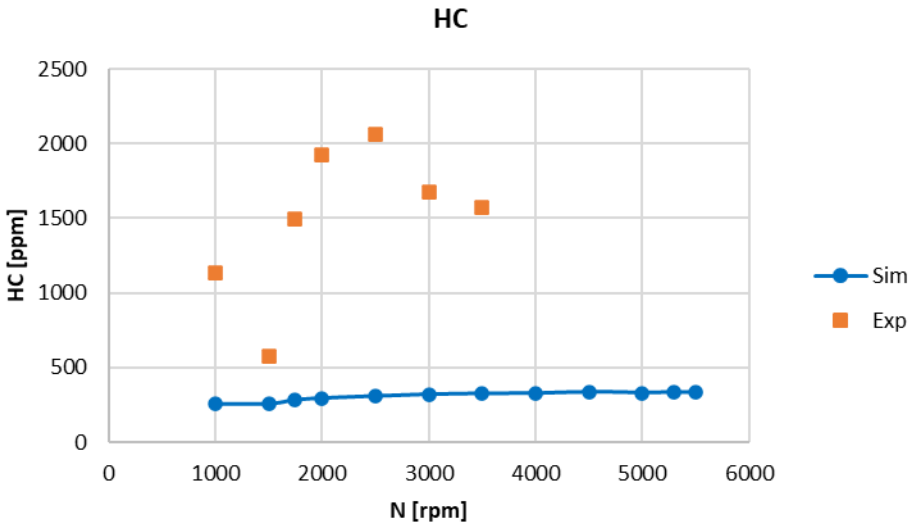

E. Estimated HC by the model for gasoline-fueled EF7TC, full load condition